Journal of Solid State Chemistry 183 (2010) 1609–1614

Contents lists available at ScienceDirect

Journal of Solid State Chemistry

journal homepage: www.elsevier.com/locate/jssc

Exploring order–disorder structural transitions in the Li–Nb–N–O system: The new antifluorite oxynitride $Li_{11}NbN_4O_2$

J. Cabana [a,1], M. Casas-Cabanas [b], H.J. Santner [a], A. Fuertes [a], M.R. Palacín [a,*]

[a] Institut de Ciència de Materials de Barcelona (CSIC), Campus UAB, E-08193 Bellaterra, Catalonia, Spain
[b] Laboratoire CRISMAT, UMR 6508 CNRS ENSICAEN, 6 bd Maréchal Juin, 14050 CAEN, France

ARTICLE INFO

Article history:
Received 18 March 2010
Received in revised form
29 April 2010
Accepted 10 May 2010
Available online 2 June 2010

Keywords:
Lithium niobium oxynitride
Neutron diffraction
Synthesis
Order–disorder

ABSTRACT

A systematic exploratory study of the Li–Nb–N–O system at low oxygen and high lithium contents has been performed. As lithium and oxygen increase, an order–disorder transition has been identified using powder neutron diffraction data between $Li_{16}Nb_2N_8O$, which crystallizes in an antifluorite-type superstructure with cationic and anionic ordering, and $Li_{11}NbN_4O_2$, a new antifluorite-type oxynitride that shows structural disorder. A description of the synthetic conditions required to prepare these phases and their structural characterization is presented.

1. Introduction

The search of new compounds showing interesting physical properties or completely new crystal structures has triggered the exploration of different mixed oxyanion systems in recent years, pushed by an improvement in the technology and know-how of both their preparation and their manipulation. Among them, oxynitrides appear specially promising [1]; different examples have been reported of phases with possible applications in photocatalysis [2–7], photoluminescence [8,9], dielectrics [10], non-toxic inorganic pigments [7,11], colossal magnetoresistance [12] or negative electrode [13,14] and electrolyte [15] materials in Li-ion batteries. Due to the structural similarities found, in some cases, with oxides, further tuning of the properties can be envisaged by designing and preparing solid solutions with controlled O/N ratios [16–21]. In addition to their composition, anion ordering in phases containing both nitride and oxide ions is also an important topic of discussion as it can affect, for instance, the transport properties [22] and behaviour as electrodes in batteries [13,23] of the resulting compounds. Extensive discussion of O/N ordering in a collection of systems is available in the literature [24–30].

Very recently, a thorough and systematic study [31] of the ordering in a collection of mixed oxyanion phases led to conclude that predictions on the distribution of the anions in a given structure could be made, with accuracies of up to 20%, by rationalizing the bond strength of each available site using Pauling's second crystal rule [32]. In brief, this states that for each anion, the charge, q, tends to be equal to the bond strength sum, b, in a given site, defined as

$$b = \sum_i \frac{z_i}{v_i}$$

where z_i is the formal oxidation state of each cation bound to a given anionic position and v_i is its coordination number.

A limited number of lithium transition metal oxynitrides have been reported to date. In fact, in some cases such as $Li_{16}M_2N_8O$ (M=Nb, Ta) [33–35], $Li_{14}Cr_2N_8O$ [36,37], $Li_6Ca_{12}Re_4N_{16}O_3$ [38] or $Li_2Sr_6Cr_2N_8O$ [39], they were discovered due to small accidental oxygen leaks in the reaction settings intended in principle for the preparation of nitrides. Although some examples with Ti and V have been synthesized by ammonolysis of oxide mixtures at high temperatures [40–42], the most common method of preparation of these phases was pioneered by Juza and co-workers in the 1950s. They investigated the possibility of controlling the amount of oxygen in lithium transition metal oxynitrides by adding variable quantities of binary oxides to a mixture with Li_3N and a transition metal, which was heated under nitrogen atmosphere. The result was a series of compounds that were formulated as solid solutions of a lithium ternary nitride containing Ti [43], V [44], Cr and Mo [45], and Li_2O. These systems have been revisited in recent years [23,36,46,47], and the approach was extended to explore new phases containing Mn [13,17,48],

* Corresponding author. Fax: +34 93 580 5731.
E-mail address: rosa.palacin@icmab.es (M.R. Palacín).
[1] Present address: Environmental Energy Technologies Division, Lawrence Berkeley National Laboratory, Berkeley, CA 94720, USA.

0022-4596/$ - see front matter © 2010 Elsevier Inc. All rights reserved.
doi:10.1016/j.jssc.2010.05.012

Nb [33,34] and Ta [35]. Most of the nitrides and oxynitrides prepared by using this procedure were shown to crystallize in an antifluorite-type structure. However, while the nitrides consistently show superstructures due to Li and M ordering, both ordered and disordered structures have been found for the oxynitrides, depending on the composition. For instance, as increasing amounts Li_2O are added to a reagent mixture to prepare Li_6CrN_4, $Li_{14}Cr_2N_8O$ [36,37], showing an antifluorite-type superstructure with Li/Cr and O/N ordering, and $Li_{10}CrN_4O_2$ [23], with a disordered structure, can be prepared. It appears that this methodology could be extended to systems with other transition metals, like Nb. While two disordered cubic NaCl-type solid solutions, $Li_{2-x}Nb_{2+x}N_{4-y}O_y$ and $Li_{1-x}Nb_{3-3x}\square_{4x}N_{4-y}O_y$ (where $\square$ = vacancy) [41,49–51], have been reported, only ordered antifluorite-type $Li_{16}Nb_2N_8O$ [33,34] has previously been synthesized in the lithium-rich part of the phase diagram. New oxynitrides showing a structurally disordered antifluorite framework could, in theory, be prepared using a nitrogen-based synthesis method by modifying the oxygen contents of the initial reagent mixtures. With this aim in mind, as reported hereafter, an exploratory study of the Li–Nb–N–O system at low oxygen and high lithium contents has been performed, which result in the preparation of a new disordered antifluorite-type oxynitride, $Li_{11}NbN_4O_2$. Earlier studies of $Li_{16}Nb_2N_8O$ have relied on single crystal X-ray diffraction to characterize the structure. However, this technique often requires complementary calculations of the Madelung part of the lattice energy (MAPLE) in order to confirm the existence of O/N ordering [52,53], due to the very similar and weak scattering factors of these two elements. Therefore, the existence of order–disorder transitions within the Li–Nb–N–O system was probed in this work using powder neutron diffraction, which can effectively resolve light elements like O and N (b_O = 5.81 fm, b_N = 9.36 fm) [54].

2. Materials and methods

Samples with different Li, Nb, N and O contents were prepared from a powder mixture of Li_3N (Sigma-Aldrich), NbN (Alfa Aesar) and Li_2O (Sigma-Aldrich, 97%) in different proportions. The samples were pelletized and heated in a tube furnace under nitrogen flow (Carburos Metálicos, 99.9995%, additionally purified with a Supelco® gas purifier). All manipulations involving air-sensitive compounds were performed in an Ar-filled glovebox.

Powder X-ray diffraction (XRD) patterns were obtained with a Rigaku Rotaflex RU-200B rotating anode diffractometer with Cu$K\alpha$ radiation (λ = 1.5418 Å), with a step size of 0.02° and 4°/min scan speed. The air- and moisture-sensitive compounds were protected during XRD measurements by covering the sample holder with a Kapton® window.

Neutron diffraction measurements were performed on high resolution D1A and D2B instruments at the Institute Laue Languevin (ILL, Grenoble, France), at λ = 1.389 and 1.6 Å, respectively, with a step size of 0.05° on a 2θ domain ranging from 1° to 150°. All Rietveld refinements were carried out with the FullProf program [55] (Windows version, April 2008) using the pseudo-Voigt profile function of Thompson et al. [56]. The instrumental resolution function (IRF) parameters used to model the instrumental contribution to the profile of the peaks are U = 0.11866 deg^2, V = −0.21449 deg^2, W = 0.16915 deg^2 for D1A instrument and U = 0.087696 deg^2, V = −0.270815 deg^2, W = 0.287651 deg^2 for D2B instrument. The background was refined by adjusting the height of pre-selected points for linear interpolation and an absorption correction was applied using a coefficient that depends on the sample's diameter.

Electrochemical lithium intercalation/deintercalation tests were performed in two-electrode Swagelok® cells using lithium foil (Aldrich 99.9%) as counter electrode. The working electrode consisted of a powder mixture of the lithium transition metal oxynitride with 15% SuperP carbon black. Two sheets of Whatman GF/D borosilicate glass fibre soaked with 1 M $LiPF_6$ in ethylene carbonate (EC):dimethylcarbonate (DMC) 1:1 electrolyte solution (Merck) were used as a separator and the cells were tested using a MacPile potentiostat (Bio-logic, France) in galvanostatic mode.

3. Results and discussion

Previous studies have shown that the synthesis of lithium transition metal nitrides and oxynitrides with high alkali and pnictide stoichiometries is not straightforward [17,23,47], and their final composition is difficult to predict. First, the partial loss of Li_2O and, especially, Li_3N through volatilization during the synthesis will affect the Li/Nb ratio in the final product, especially considering that this loss will depend on the reaction conditions (i.e., temperature and time). Second, the nitrogen content in the final product will be higher than that in the reaction mixture, as some nitrogen gas is reduced to nitride through the oxidation of a transition metal like niobium, which has a strong tendency to form compounds in which its oxidation state is +5. For this reason, the synthesis attempts made through the course of this work required not only the control of the oxygen content by adding amounts of Li_2O, but also the compensation of the different losses of lithium in the range of temperatures explored for the preparation of single-phase samples by tuning the Li/Nb ratio through the change of the initial Li_3N contents.

The XRD patterns resulting from the heat treatment (at 700 °C ≤ T ≤ 900 °C) of mixtures of only Li_3N and NbN (with 9 ≥ Li/Nb ≥ 7.25) show that these samples invariably are, contrary to what would be expected, multi-phase and contain both the ternary nitride, Li_7NbN_4 [57], and $Li_{16}Nb_2N_8O$ (Fig. 1a). Note that the high background level observed at $2\theta < 30°$ and the large shoulder centred at 2θ = 26° (marked with an asterisk) are due to the

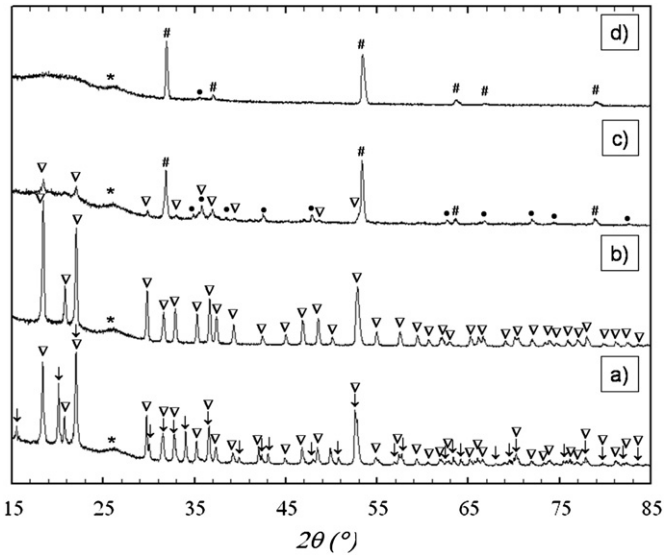

Fig. 1. X-ray diffraction patterns of mixtures of Li_3N, Li_2O, and NbN in diverse ratios treated at 800–900 °C for 4–6 h: (a) T = 800 °C, t = 4 h, Li/Nb = 8; (b) T = 850 °C, t = 4 h, Li/Nb = 9.36, O/Nb = 0.18; (c) T = 800 °C, t = 6 h, Li/Nb = 8.25, O/Nb = 0.5; and (d) T = 820 °C, t = 4 h, Li/Nb = 19, O/Nb = 2. The resulting products are mixtures of the ordered antifluorite-type $Li_{16}Nb_2N_8O$ phase (▽), a phase with a cubic antifluorite structure (#) and NbN (●) in diverse proportions depending mainly on the O/Nb starting ratio.

Kapton® foil used to protect the samples from air and moisture during the measurements. Pure $Li_{16}Nb_2N_8O$ could be prepared when a mixture of 3 mole Li_3N, 1 mole NbN and 0.18 mole Li_2O was heated at 850 °C for 4 h (Fig. 1b). Lower Li/Nb (several ratios down to stoichiometric were tested), and both lower (800 °C) and higher (900 °C) temperatures of reaction always led to the presence of NbN in the final product. The need to start with a Li/Nb ratio that is slightly higher than stoichiometric proves the need to initially add an excess of Li_3N to compensate for some evaporation at high temperatures. The existence of a higher proportion of oxygen than initially added in these samples suggests that very small impurities of this element cannot be avoided. Such impurities are generated either from the nitrogen gas supply, even when using a purifier, or are due to small leaks in the tube furnace setup with continuous gas flow required to prepare this nitrogen-rich phases.

Previous crystal-chemical characterization of $Li_{16}Nb_2N_8O$ was performed using X-ray radiation data [33,34]. With the aim of confirming the existence of ordering for light elements such as O, N or Li, which have weak X-ray scattering factors, neutron powder diffraction data from the D2B instrument in ILL was refined instead, using the structure reported from single crystal XRD as a starting point [33,34]. A small peak around 25°, which belongs to an unidentified impurity that was also found during the course of the exploration of the Li–Cr–N–O system [23], was excluded from the refinement. Cell parameters, atomic positions, atomic displacement factors, pseudo-Voigt profile parameters and background points were refined simultaneously. However, the isotropic displacement factors of the same type of elements had to be constrained to obtain a stable refinement. The final Rietveld refined fit is shown in Fig. 2 and the resulting crystallographic parameters are listed in Tables 1 and 2. As previously reported [33,34], and as shown as an inset in Fig. 2, $Li_{16}Nb_2N_8O$ crystallizes in an antifluorite-type superstructure in which both lithium and niobium atoms are tetrahedrally coordinated, and oxygen and nitrogen are located in cubic sites. A list of selected bond distances is shown in Table 3. The transition metal atoms are only coordinated by nitrogen atoms, with an average distance of 1.98 Å. On the other hand, the lithium atoms are either surrounded by nitrogen atoms only (Li(1) and Li(4)), with an average distance of 2.18 Å, or by both nitrogen and oxygen (Li(2) and Li(3)), with an average Li–N distance of 2.19 Å and an average

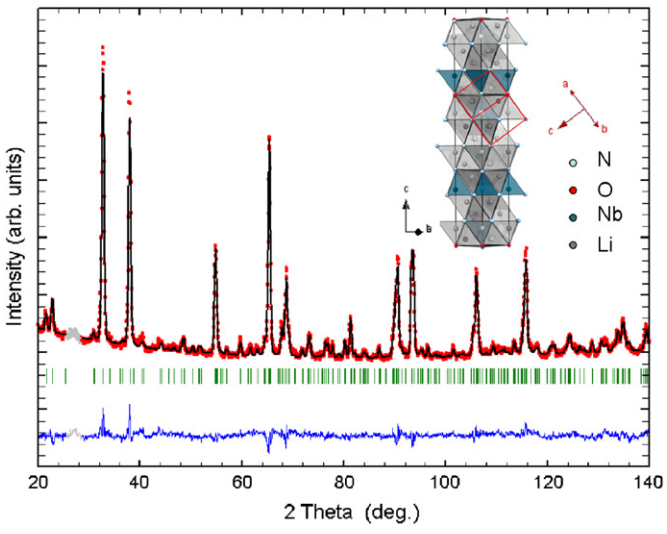

Fig. 2. Neutron powder diffraction pattern (small circles) showing the final Rietveld fit (solid line), with the difference plot below for $Li_{16}Nb_2N_8O$. Inset: Polyhedral representation of the final refined unit cell and its relationship to the antifluorite type cell (in red). (For interpretation of the references to colour in this figure legend, the reader is referred to the web version of this article.)

Table 1
Rietveld refinement details for $Li_{16}Nb_2N_8O$ and $Li_{11}NbN_4O_2$. The number of refined parameters corresponds to the whole diffraction pattern including cell parameters of the impurities present. Resulting agreement factors are background-corrected to avoid misleading low values derived from the low signal-to-noise ratio [62].

Crystal system	Rhombohedral	Cubic
Space group	$R\bar{3}$	$FM\bar{3}M$
a (Å)	6.0043(2)	4.8098(2)
c (Å)	25.606(1)	
V (Å^3)	799.47(2)	111.270(4)
Radiation type	Neutron	Neutron
Instrument	D2B	D1A
Wavelength (Å)	1.6	1.389
2θ range (deg)	1–150	1–150
2θ increment (deg)	0.05	0.1
excluded regions (deg)	25.50–28.40	–
R_p	18.9	47.0
R_{wp}	15.5	24.5
R_{Bragg}	7.93	5.09
χ^2	0.71	1.21
No. of Bragg reflections	366	18
No. of refined parameters	35	17

Table 2
Atomic positions and thermal displacements for $Li_{16}Nb_2N_8O$.

	Wyckoff site	x	y	z	B (Å^2)
Nb	6*c*	0	0	0.2485(7)	0.1(2)
N1	18*f*	0.311(1)	0.314(1)	0.2244(5)	0.77(9)
N2	6*c*	0	0	0.3265(4)	0.77(9)
O	3*a*	0	0	0	0.6(5)
Li1	18*f*	0.359(9)	0.308(9)	0.474(1)	1.2(3)
Li12	18*f*	0.03(1)	0.333(8)	0.028(2)	1.2(3)
Li3	6*c*	0	0	0.079(3)	1.2(3)
Li4	6*c*	0	0	0.412(3)	1.2(3)

Table 3
Selected atomic distances for $Li_{16}Nb_2N_8O$.

Atom 1	Atom 2	Distance (Å)
Nb1	N1	1.973(4) × 3
Nb1	N2	1.997(9)
Li1	N1	2.07(2)
Li1	N1	2.14(2)
Li1	N1	2.16(2)
Li1	N1	2.31(3)
Li2	O1	2.05(2)
Li2	N1	2.10(2)
Li2	N2	2.12(2)
Li2	N2	2.23(3)
Li3	O1	2.01(3)
Li3	N1	2.23(1) × 3
Li4	N1	2.19(9) × 3
Li4	N2	2.20(3)

Li–O distance of 2.03 Å. These values are in full agreement with the sum of the effective ionic radii tabulated by Shannon [58] and Baur [59] for oxides and nitrides, respectively, which predict and average Li–O bond distance of 2.01 Å and a Li–N bond distance of 2.16 Å. The refined values of cell parameters (a=6.0043(2) Å and c=25.606 (1) Å) are slightly higher than those resulting from the refinement of single crystal XRD data, reported by Chen and Eick [33] (a=5.984(4) Å and c=25.484 Å). These differences could be attributed to slight differences in lithium and oxygen content, as different reaction conditions were used in both cases. Sensitivity

of the unit cell volume to these contents has been reported for similar oxynitride systems [17,23,46,47].

When the initial Li_2O content is increased with respect to the amounts empirically found to lead to $Li_{16}Nb_2N_8O$, a concomitant and sharp increase in the relative intensity of the XRD peaks at 32° and 53.5° is observed (see a representative pattern of this phenomenon in Fig. 1c). Similar behaviour has previously been described for related systems with Mn, Cr, V and Ti [17,23,47] and is an indication of the formation of a new lithium niobium oxynitride with higher lithium and oxygen contents. This new oxynitride crystallizes in a simple cubic antifluorite structure, which is the fingerprint of structural cationic and anionic disorder within the framework [17,23,43–47]. To the best of our knowledge, the existence of such phase is described here for the first time. In order to obtain single-phase samples, a complete survey of reaction conditions and initial stoichiometries was performed. It was found that, while heat treatment temperatures below 800 °C consistently led to the presence of unreacted starting compounds, excessive lithium evaporation at 900 °C produced samples that always contained considerable amounts of NbN; the optimum temperature was found to be in the narrow range between 820 and 850 °C. The length of the heat treatment proved to have similar effects; while relatively pure samples were obtained after 4 h, shorter (1–3 h) and longer (6–8 h) treatments favoured the presence, respectively, of unreacted reagents and of NbN due to excessive lithium evaporation. Unsuccessful attempts to compensate the latter were made by increasing the initial Li_3N amounts; noticeable amounts of impurities where observed even when Li_3N:NbN was set to 6:1.

The initial proportions of each of the three reagents was also found to have an important role in the purity of the samples; as the Li_2O amount is increased, a subsequent increase of the Li_3N was required to avoid large NbN impurities. Such need for compensating amounts of Li_3N as more Li_2O is added to a mixture to produce lithium transition metal oxynitrides has also been reported in other related systems with Mn and Cr [17,23]. Finally, lithium niobium oxynitride showing a simple cubic antifluorite structure could be prepared by heating a mixture with Li/Nb=9 and O/Nb=2 at 820 °C for 4 h (Fig. 1d). Only a very small amount of NbN was detected by XRD in these conditions. Less pure samples with O/Nb=1 and 3 were also synthesized. Although an accurate determination of their cell parameters with respect to composition is hindered by the presence of secondary phases, a tendency for a shift of the peaks to higher 2θ with higher O/Nb was observed, which is an indication of the reduction of the unit cell volume as the transition metal and nitrogen are diluted with lithium and oxygen. This is driven by the rather smaller ionic radius of O^{2-} as opposed to N^{3-} [58,59] and is again in agreement with previous studies [17,23,43–47,60].

Neutron powder diffraction data of this new lithium niobium oxynitride were collected using the D1A high-resolution powder diffractometer. Due to the large amounts of sample required for a neutron experiment and the small scale of the synthesis procedure necessary to produce good purity samples (typically, 500 mg are obtained per pellet), a sample prepared by mixing two batches was initially measured. Unfortunately, the sample was found to consist of two phases with very slightly different cell parameters, indicating subtle differences in composition (see Fig. S1 in the Supplementary Materials) even though the synthetic conditions used to prepare the two batches were identical. All attempts to prepare a large enough sample by grouping different batches resulted unfruitful, systematically leading to mixtures of slightly different compositions. Together with the narrow window of reaction temperature and time at which pure samples could be obtained (see above), these difficulties reveal the delicate equilibria that govern the Li–Nb–N–O system. In order to characterize the crystal chemistry of a single lithium niobium oxynitride, a neutron experiment was performed with a slightly larger, single batch sample, at the expense of a lower signal-to-noise ratio. Small amounts of Li_2O (powder diffraction file-PDF-card 12-254, $Fm\bar{3}\ m$ space group, $a=4.6168(9)$ Å) and two different polytypes of NbN (PDF cards 20-801, $P6_3/mmc$ space group, $a=2.9603(2)$ Å and $c=11.273(2)$ Å, and 74-780, $I4/mmm$ space group, $a=4.3908(9)$ Å and $c=8.624(2)$ Å), which are likely the result of their relative phase stability at the temperatures of synthesis [61], were detected in the diffraction pattern and were included in the refinement in profile matching mode. Taking the O/Nb ratio of 2 used in the starting mixture and assuming a vacancy-free structure containing Nb^{5+}, as in parent $Li_{16}Nb_2N_8O$, the composition $Li_{11}NbN_4O_2$ was chosen as starting point for the refinement of the crystal structure of the majority phase. Cell parameters, atomic displacement factors, pseudo-Voigt profile parameters and background points were refined simultaneously. Attempts to refine the atomic occupancies were unsatisfactory due to a too low signal-to-noise ratio. Nonetheless, this nominal composition fits the data well (Fig. 3). The resulting Rietveld refinement details and atomic parameters are listed in Tables 1 and 4, respectively. The average structure, shown as an inset in Fig. 3, corresponds to a disordered antifluorite in which lithium atoms and niobium atoms are tetrahedrally coordinated either to oxygen or nitrogen atoms. In turn, nitrogen and oxygen occupy the 8*c* sites and are 8-coordinated by cations. The average cation–anion distance is 2.08 Å, which is consistent with the average cation–anion distance in the ordered antifluorite $Li_{16}Nb_2N_8O$.

It has previously been shown that nitride ions in ordered oxynitrides have a tendency to occupy the anion sites with larger coordination numbers or to bond to a larger number of small cations with high oxidation states, thereby satisfying of the Pauling's second crystal rule (PSCR) [30,31]. As a consequence, in ordered oxynitrides containing transition metals and electropositive elements (alkaline, alkaline earth or rare-earth metals)

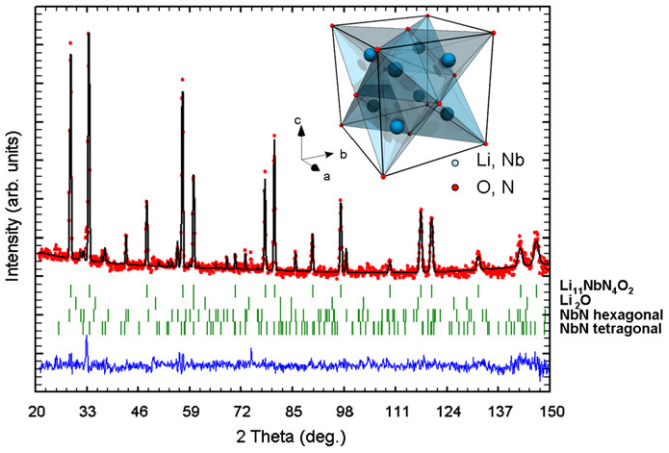

Fig. 3. Neutron powder diffraction patterns (small circles) showing the final Rietveld fit (solid line), with the difference plot below for $Li_{11}NbN_4O_2$. Inset: Polyhedral representation of the average refined unit cell.

Table 4
Atomic positions and thermal displacements for $Li_{11}NbN_4O_2$.

	Wyckoff site	*x*	*y*	*z*	*B* (Å^2)
Li/Nb	8*c*	0.25	0.25	0.25	1.8(2)
N/O	4*a*	0	0	0	1.00(6)

nitrogen occupies the sites showing a larger number of bonds to transition metals than those corresponding to oxygen positions. This trend is applicable to the ordered oxynitrides $Li_{16}Nb_2N_8O$ and $Li_{16}Ta_2N_8O$ (isostructural), $Li_{14}Cr_2N_8O$, $Li_6Ca_{12}Re_4N_{16}O_3$ and $Li_2Sr_6Cr_2N_8O$, where the transition metal is bonded preferentially to nitrogen, in agreement with PSCR. In the antifluorite-type $Li_{16}M_2N_8O$ (M=Nb or Ta) and $Li_{14}Cr_2N_8O$, the nitrogen atoms are coordinated to 7 and 6 lithium atoms, respectively, and to one transition metal, whereas oxygen always occupies sites with CN=8 that are only surrounded by lithium atoms. In all cases, the resulting bond strength sums (b) for nitrogen and oxygen sites are 3 and 2, respectively, which is also in agreement with PSCR ($q=b$ for both sites). In contrast, the disordered antifluorite $Li_{10}CrN_4O_2$ shows both N and O in 8-coordinated 8c site with b sums of 2.67 (average q for this site=2.67). It should be pointed that in a disordered mixed anion compound showing one anion site, b is always equal to q. The increase in the oxygen content (and in Li content) from $Li_{14}Cr_2N_8O$ to $Li_{10}CrN_4O_2$ stabilizes the disordered structure with $b=q$ for the unique anion position. A similar behaviour has been shown here for the Li–Nb–N–O system, where $Li_{16}Nb_2N_8O$ shows an ordered structure with niobium preferentially coordinated by nitrogen, whereas $Li_{11}NbN_4O_2$ is disordered.

The cationic vacancies in the antifluorite structure of disordered lithium transition metal oxynitrides with Mn and Cr could reversibly be filled by Li^+ when these compounds were tested in a lithium battery [13,23]. When no such vacancies are present, as is the case of the phases containing Ti and V, no electroactivity was observed [47]. The absence of vacancies in the structure of the lithium niobium oxynitrides prepared here, as indicated, for instance, by the 2-to-1 ratio of cations to anions in $Li_{11}NbN_4O_2$, was indirectly confirmed by the absence of electrochemical activity toward lithium intercalation.

4. Conclusions

A systematic exploratory study of the Li–Nb–N–O system at low oxygen and high lithium contents has been performed. High purity phases were only obtained in a narrow window of experimental conditions. $Li_{16}Nb_2N_8O$ could be prepared when a mixture of 3 mole Li_3N, 1 mole NbN and 0.18 mole Li_2O was heated at 850 °C for 4 h. The refinement of powder neutron diffraction data confirmed that, as indicated by earlier X-ray diffraction studies, this phase crystallizes in an antifluorite-type superstructure with cationic and anionic order, in which the niobium and oxygen atoms are only coordinated by nitrogen and lithium atoms, respectively. As lithium and oxygen increase, an order–disorder transition has been identified. A new phase, $Li_{11}NbN_4O_2$, was prepared by heating a Li_3N, Li_2O and NbN mixture with Li/Nb=9 and O/Nb=2 at 820 °C for 4 h. The results of Rietveld refining powder neutron diffraction data indicate that this new oxynitride crystallizes in a simple antifluorite structure, with disorder in both cationic and anionic positions. None of these lithium niobium oxynitrides was found to have any vacancies in their framework, as proved by their inactivity toward electrochemical lithium intercalation.

Acknowledgments

The authors would like to thank J. Rodriguez-Carvajal for useful discussions and for help in the acquisition of neutron diffraction data. This work was supported by Ministerio de Ciencia e Innovación (MAT2008-04587).

Appendix. Supplementary Material

Supplementary data associated with this article can be found in the online version at doi:10.1016/j.jssc.2010.05.012.

References

[1] A. Fuertes, Dalton Trans. , doi:10.1039/c000502a.
[2] R. Asahi, T. Morikawa, T. Ohwaki, K. Aoki, Y. Taga, Science 293 (2001) 269.
[3] G. Hitoki, T. Takata, J.N. Kondo, M. Hara, H. Kobayashi, K. Domen, Chem. Commun. (2002) 1698.
[4] K. Maeda, K. Teramura, D.L. Lu, T. Takata, N. Saito, Y. Inoue, K. Domen, Nature 440 (2006) 295.
[5] E. Martinez-Ferrero, Y. Sakatani, C. Boissiere, D. Grosso, A. Fuertes, J. Fraxedas, C. Sanchez, Adv. Funct. Mater. 17 (2007) 3348.
[6] A.B. Jorge, J. Fraxedas, A. Cantarero, A.J. Williams, J. Rodgers, J.P. Attfield, A. Fuertes, Chem. Mater. 20 (2008) 1682.
[7] F. Tessier, P. Maillard, F. Chevire, K. Domen, S. Kikkawa, J. Ceram. Soc. Jpn. 117 (2009) 1.
[8] E. Soignard, D. Machon, P.F. McMillan, J.J. Dong, B. Xu, K. Leinenweber, Chem. Mater. 17 (2005) 5465.
[9] V. Bachmann, C. Ronda, O. Oeckler, W. Schnick, A. Meijerink, Chem. Mater. 21 (2009) 316.
[10] Y.I. Kim, P.M. Woodward, K.Z. Baba-Kishi, C.W. Tai, Chem. Mater. 16 (2004) 1267.
[11] M. Jansen, H.P. Letschert, Nature 6781 (2000) 980.
[12] A.B. Jorge, J. Oro-Sole, A.M. Bea, N. Mufti, T.T.M. Palstra, J.A. Rodgers, J.P. Attfield, A. Fuertes, J. Am. Chem. Soc. 130 (2008) 12572.
[13] J. Cabana, N. Dupré, C.P. Grey, G. Subias, M.T. Caldés, A.M. Marie, M.R. Palacín, J. Electrochem. Soc. 152 (2005) A2246.
[14] J. Cabana, C.M. Ionica-Bousquet, C.P. Grey, M.R. Palacín, Electrochem. Commun. 12 (2010) 315.
[15] J.B. Bates, N.J. Dudney, G.R. Gruzalski, R.A. Zuhr, A. Choudhury, C.F. Luck, J.D. Robertson, J. Power Sources 43 (1993) 103.
[16] K. Maeda, K. Domen, J. Phys. Chem. C 111 (2007) 7851.
[17] J. Cabana, N. Dupré, F. Gillot, A.V. Chadwick, C.P. Grey, M.R. Palacín, Inorg. Chem. 48 (2009) 5141.
[18] O. Morey, P. Goeuriot, D. Juve, D. Treheux, J. Eur. Ceram. Soc. 23 (2003) 345.
[19] N. Diot, O. Larcher, R. Marchand, J.Y. Kempf, P. Macaudière, J. Alloys Compd. 323–324 (2001) 45.
[20] A. Kusmartseva, M. Yang, J. Oro-Sole, A.M. Bea, A. Fuertes, J.P. Attfield, Appl. Phys. Lett. 95 (2009) 022110.
[21] M. Yang, J. Oró-Solé, A. Kusmartseva, A. Fuertes, J.P. Attfield, J. Am. Chem. Soc. 132 (2010) 4822.
[22] G. Tobías, E. Canadell, J. Am. Chem. Soc. 128 (2006) 4318.
[23] J. Cabana, C.D. Ling, J. Oró-Solé, D. Gautier, G. Tobías, S. Adams, E. Canadell, M.R. Palacín, Inorg. Chem. 43 (2004) 7050.
[24] P.L. Wang, P.E. Werner, L.A. Gao, R.K. Harris, D.P. Thompson, J. Mater. Chem. 7 (1997) 2127.
[25] S.J. Clarke, C.W. Michie, M.J. Rosseinsky, J. Solid State Chem. 146 (1999) 399.
[26] C.M. Fang, G.A. de Wijs, R.A. de Groot, R. Metselaar, H.T. Hintzen, G. de With, Chem. Mater. 12 (2000) 1071.
[27] C.M. Fang, E. Orhan, G.A. de Wijs, H.T. Hintzen, R.A. de Groot, R. Marchand, J.-Y. Saillard, G. de With, J. Mater. Chem. 11 (2001) 1248.
[28] S.J. Clarke, K.A. Hardstone, C.W. Michie, M.J. Rosseinsky, Chem. Mater. 14 (2002) 2664.
[29] C.F. Baker, M.G. Barker, C. Wilson, D.H. Gregory, Dalton Trans. (2004) 1298.
[30] G. Tobías, D. Beltrán-Porter, O.I. Lebedev, G. Van Tendeloo, J. Rodriguez-Carvajal, A. Fuertes, Inorg. Chem. 43 (2004) 8010.
[31] A. Fuertes, Inorg. Chem. 45 (2006) 9640.
[32] L. Pauling, J. Am. Chem. Soc. 51 (1929) 1010.
[33] X.Z. Chen, H.A. Eick, J. Solid State Chem. 127 (1996) 19.
[34] C. Wachsmann, H. Jacobs, Z. Kristallogr. 211 (1996) 477.
[35] C. Wachsmann, T. Brokamp, H. Jacobs, J. Alloys Compd. 185 (1992) 109.
[36] A. Gudat, S. Haag, R. Kniep, A. Rabenau, Z. Naturforsch. B 45 (1990) 111.
[37] T.M. Akhmetzyanov, V.P. Obrosov, N.N. Batalov, S.V. Plaksin, Z.S. Martem'yanova, V.K. Tamm, Russ. J. Electrochem. 29 (1993) 1187.
[38] O. Hochrein, R. Kniep, Z. Anorg. Allg. Chem. 627 (2001) 301.
[39] O. Hochrein, R. Kniep, Z. Anorg. Allg. Chem. 628 (2002) 1.
[40] R. Assabaa-Boultif, R. Marchand, Y. Laurent, Eur. J. Solid State Inorg. Chem. 32 (1995) 1101.
[41] R. Assabaa-Boultif, R. Marchand, Y. Laurent, Ann. Chim.-Sci. Mater. 19 (1994) 39.
[42] T. Katsumata, S. Takaki, Y. Inaguma, Y.J. Shan, Solid State Commun. 132 (2004) 583.
[43] R. Juza, W. Uphoff, W. Gieren, Z. Anorg. Allg. Chem. 292 (1957) 71.
[44] R. Juza, W. Gieren, J. Haug, Z. Anorg. Allg. Chem. 300 (1959) 61.
[45] R. Juza, J. Haug, Z. Anorg. Allg. Chem. 309 (1961) 276.
[46] R. Niewa, D. Zherebtsov, Z. Hu, Inorg. Chem. 42 (2003) 2538.
[47] J. Cabana, C. Mercier, D. Gautier, M.R. Palacín, Z. Anorg. Allg. Chem. 631 (2005) 2136.

[48] J. Cabana, G. Rousse, A. Fuertes, M.R. Palacín, J. Mater. Chem. 13 (2003) 2402.
[49] F. Tessier, R. Assabaa, R. Marchand, J. Alloys Compd. 262-263 (1997) 512.
[50] F. Tessier, R. Marchand, Y. Laurent, J. Eur. Ceram. Soc. 17 (1997) 1825.
[51] R. Marchand, F. Tessier, F.J. DiSalvo, J. Mater. Chem. 9 (1999) 297.
[52] R. Lauterbach, W. Schnick, Z. Anorg. Allg. Chem. 624 (1998) 1154.
[53] R. Lauterbach, E. Irran, P.F. Henry, M.T. Weller, W. Schnick, J. Mater. Chem. 10 (2000) 1357.
[54] H. Rauch, W. Waschkowski, Landolt–Börnstein: numerical data and functional relationships in science and technology, in: Schopper H. (Ed.), Low Energy Neutrons and their Interaction with Nuclei and Matter, 1, Springer, Berlin, 2000, p. 1 (Chapter 6).
[55] J. Rodríguez-Carvajal, Physica B 192 (1993) 55.
[56] P. Thompson, D.E. Cox, J.B. Hastings, J. Appl. Crystallogr. 20 (1987) 79.
[57] D.A. Vennos, F.J. DiSalvo, Acta Crystallogr. C 48 (1992) 610.
[58] R.D. Shannon, Acta Crystallogr. A32 (1976) 751.
[59] W.H. Baur, Cryst. Rev 1 (1987) 59.
[60] R. Niewa, R. Kniep, Z. Kristallogr. NCS 216 (2001) 5.
[61] W. Lengauer, M. Bohn, B. Wollein, K. Lisak, Acta Mater. 48 (2000) 2633.
[62] R.J. Hill, R.X. Fischer, J. Appl. Crystallogr. 23 (1990) 462.